Desalination and Water Treatment
www.deswater.com

doi: 10.5004/dwt.2022.28864

273 (2022) 221–235
October

Application of NaOH modified rice husk as a potential sorbent for removal of Congo red from an aqueous solution

Muhammad Imran Khan[a,*], Abdallah Shanableh[a], Noureddine Elboughdiri[b,c], Suryyia Manzoor[d], Sidra Mubeen[e], Aziz ur Rehman[f]

[a]*Research Institute of Sciences and Engineering (RISE), University of Sharjah, Sharjah 27272, United Arab Emirates, emails: raoimranishaq@gmail.com/mimran@sharjah.ac.ae (M.I. Khan), shanableh@sharjah.ac.ae (A. Shanableh)*
[b]*Chemical Engineering Department, College of Engineering, University of Ha'il, P.O. Box: 2440, Ha'il 81441, Kingdom of Saudi Arabia, email: ghilaninouri@yahoo.fr*
[c]*Chemical Engineering Process Department, National School of Engineering Gabes, University of Gabes, Gabes 6011, Tunisia*
[d]*Institute of Chemical Sciences, Bahauddin Zakariya University, Multan 60800, Pakistan, email: suryyia.manzoor@bzu.edu.pk*
[e]*Department of Chemistry, The Women University Multan, Katchery Campus, LMQ Road, Multan, email: sidra_sidra786@yahoo.com*
[f]*Institute of Chemistry, The Islamia University of Bahawalpur, Bahawalpur 63100, Pakistan, email: azizypk@yahoo.com*

Received 23 February 2022; Accepted 18 August 2022

ABSTRACT

Due to the prevailing treacherous impacts of dyes on aquatic as well as terrestrial ecosystems, the designing of cost effective and facile removal methods are utmost need of time. The current research encompasses the study of modified rice husk (MRH) as an efficient adsorbent for the abatement of Congo red (CR), an anionic dye from an aqueous solution. Fourier transform infrared (FTIR) confirmed adsorption of CR onto MRH. Morphology of rice husk before and after modification was investigated by using scanning electron microscopy (SEM). Moreover, a prominent increase in surface area and porosity occurred through chemical treatment of rice husk. The effect of various factors including contact time, mass of MRH (dosage), initial concentration of CR in an aqueous solution, temperature and pH on CR adsorption was explored. Adsorption of CR was studied by using several isotherm models including Langmuir, Freundlich, Temkin and Dubinin–Radushkevich (D–R). Results showed that CR adsorption onto MRH fitted well to Freundlich isotherm. Adsorption kinetics for CR adsorption was revealed by applying many models such as pseudo-first-order, pseudo-second-order, Elovich model, modified Freundlich equation, and Bangham equation. Obtained results showed that CR adsorption from an aqueous solution onto MRH obeyed pseudo-second-order model. Adsorption thermodynamics result showed that CR adsorption onto MRH was exothermic process ($\Delta H^\circ = -4.75$ kJ/mol). The maximum adsorption capacity of 10.13 mg/g was found.

Keywords: Exothermic process; Batch adsorption; Modified rice husk; Pseudo-second-order model; Freundlich isotherm

1. Introduction

In fact water is the most significant natural resource on earth. Water pollution results when a water body is influence by huge quantities of material. Water is regarded as polluted water when it is not convenient for the deliberated applications. Hence, recognizing the kinds of pollutants existed in the water is a significant initial stage in solving this issue. The entrance of minerals, organic chemicals, or by the entrance of solid wastes into the water results to contamination in water. These chemicals enter into the water during the entry of chemical, industrial, human, household, hospital, agricultural, and other wastewater [1–4].

---

* Corresponding author.

The removal of dye from wastewaters is one of the crucial requirements in recent years [5,6]. The discharge of dye wastewaters in the ecosystem is highly harmful resulting serious threat for human being [7–9]. Even minute concentrations can cause prominent physical and chemical variation in characteristics of water and limit the aquatic life. When introduced to aquatic reservoirs, they further reduce the light's penetration and oxygen's concentration [10]. Many of the dyes act as mutagens and are carcinogenic [11]. Congo red (CR) is one of the anionic diazo dye. It has found large scale applications in pigment industries and wood manufacturing, and lead to some diseases including anorexia, gastrointestinal irritation, and weakness [4,12]. It is also studied as a mutagen and reproductive effector. CR is employed as a laboratory aid in studying for free hydrochloric acid in gastric contents, as an indicator of pH, in the diagnosis of amyloidosis, and also as a histological stain for amyloid. It has a strong affinity to cellulose fibers and thus is employed in textile industries. It is a derivative of benzidine and napthoic acid and metabolizes to carcinogenic products [13]. It may affect blood factors such as clotting, and induce somnolence and respiratory problems [14]. Therefore, the removal of CR from the wastewaters of these industries is highly essential.

Until now, several methods including chemical methods, physical methods, and biological methods were used for treatment of wastewaters which contain dyes [15–20]. Adsorption is the mostly used method among them [21]. It is one of the largely utilized methods for the removal of both inorganic [22] and organic pollutants [23] from polluted water. Based on the different interaction forces between the adsorbent and the adsorbate, it can be divided into chemical adsorption and physical adsorption [24]. The chemical adsorption results through the formation of chemical bonds or surface coordination compounds by adsorbate molecules and adsorbents by means of ion exchange, electron migration or electron pair sharing [25,26] while physical adsorption occurs due to the intermolecular forces (e.g., Van der Waals forces) [27].

Mostly used adsorbents are activated carbon, metal and non-metal oxides. Activated carbon is excellent adsorbent and possesses higher adsorption performance. Its drawbacks include higher price and the lower mechanical strength. In past several materials such as biochars from crop residues [28], walnut husk [29], biomass of penicillium YWO1 [30], composites [31], natural clinoptilolite [32], activated carbon [33], cross-linked succinyl chitosan [34], sesame hull [35], natural zealite [36], modified bentonite [37], dehydrated beet pulp carbon [38], eucalyptus barks [39], modified attapulgite [40], polyurethane foam [41], clay material [42–44], modified fungi [45] etc. have been employed as adsorbents for the discharge of dyes from an aqueous solutions. Agriculture by-products showed their capability as low cost adsorbents and are commonly modified chemically to enhance their adsorption efficiency toward dyes [46]. In addition, there are some adsorbents that present poor adsorption capacity for the anionic dyes due to their anionic or hydrophobic surfaces. Further, the regeneration of used sorbents is another challenging step that limits their use on large-scale. Such adsorbents when disposed of, also result in environmental issues [47]. Therefore, it is of higher interest to find low price and potential adsorbent for CR removal from an aqueous solution.

Previously, we reported adsorption of dyes and heavy metal ions by using different adsorbents [48–50]. In this article, batch adsorption of CR from an aqueous solution onto NaOH modified rice husk (MRH) at room temperature was reported. The effect of operating factors onto the CR percentage removal from an aqueous solution and adsorption capacity was studied. FTIR was used to confirm CR adsorption on MRH. Morphology of rice husk was revealed by scanning electron microscopy. Adsorption isotherms, kinetics and thermodynamics for CR adsorption from an aqueous solution onto MRH were also reported.

2. Experimental

2.1. Materials

Anion dye Congo red (CR) and sodium hydroxide (NaOH) were purchased from Sinopharm Chemical Reagent Co., Ltd., Shanghai, China. All chemicals were employed as received from company. Distilled water was used throughout this research. The chemical structure CR is shown in Fig. S1.

2.2. Adsorbent

Husk of basmati rice was received from the rice mill, Punjab, Pakistan. It was washed with distilled water to remove dust particle. Then it was oven dried at 80°C till constant weight was attained. Its chemical analysis was carried out by applying neutron activation analysis (NAA) and atomic adsorption spectrometry (AAS) for their trace metal contents as reported in our previous work [51]. Results showed that the quantity of metals such as Na, K, Pb and Fe were present in µg per g of sample. Silica contents were found to be 18.27 (0.62%) of TRH [51,52]. Its small amount was investigated via standard methods. Table 1 shows the concentration trace elements present in Pakistani rice husk.

2.3. Modification of RH with NaOH

It was modified by soaking the dried and washed rice husk into 1.0 M NaOH solution. Initially, 50 g of rice husk was soaked into 1.0 M NaOH solution into a 1.0 L beaker. The mixture was stirred vigorously for 24 h. After that it was washed with distilled water until neutral pH was obtained. Lastly, it was dried at 80°C in an oven till constant weight was achieved and stored in airtight container and denoted as modified rice husk (MRH).

2.4. Adsorption of CR from an aqueous solution onto MRH

Adsorption of CR from an aqueous solution onto MRH was investigated as reported in our previous work (Section S1 for detail in supporting information) [49,53–55].

2.5. Characterization

2.5.1. FTIR test

FTIR spectrometer (Vector 22, Bruker) having resolution of 2 cm^{-1} and total spectral range of 4,000–400 cm^{-1} was

Table 1
Trace elements concentration (μg/g) in Pakistani rice husk determined by NAA and AAS

Elements	Range	Median
Hg	0.141–0.436	0.39
Cd**	28–140	34
Pb**	1.56–3.48	2.22
As	0.12–0.19	0.147
Sb	0.016–6.8	0.99
Ni	0.20–2.29	0.73
Se	0.125–0.176	0.15
Br	5.52–9.8	6.7
Al	75.5–122	92
Cs*	18–55	22
Fe	99–154	125
Cu	3.8–8.1	4.3
Zn	10.6–18.4	14.4
Mn	32.2–95	74
Cr*	188–465	312
Co*	73–194	114
V	0.56–1.20	0.65
Cl	1,865–7,373	2,891
Na	109–586	204
K	2,500–62,00	5,201
Rb	1.8–2.7	2.2
Sc*	14–44	27

*Concentration expressed in ng/g;
**Determined by AAS.

employed to study MRH before and after CR adsorption by utilizing attenuated total reflectance (ATR). Morphology of RH before and after modification with NaOH was investigated by scanning electron microscopy (SEM).

2.6. Adsorption isotherms

Adsorption isotherms including Langmuir, Freundlich, Temkin and Dubinin–Radushkevich (D–R) were used to explore experimental data for CR adsorption from an aqueous solution onto MRH (Section S2 for detail in supporting information).

2.7. Adsorption kinetics

Adsorption kinetics for CR adsorption from an aqueous solution onto MRH was explored by using several kinetic models (Section S3 for detail in supporting information).

2.8. Thermodynamics study

We calculated the change in Gibb's free energy ($\Delta G°$), enthalpy ($\Delta H°$) and entropy ($\Delta S°$) for CR adsorption from an aqueous solution onto MRH to reveal adsorption thermodynamics as reported [53,56,57] (Section S4 for detail in supporting information).

3. Results and discussion

Biomasses are not only considered a cost effective approach but are also facile to use for pollutants abatement. These materials when thermally or chemically treated are capable of binding with the pollutants through van der waals forces, hydrogen bonding, ion exchange, etc. The modified rice husk was able to adsorb CR dye possibly due to hydrogen bonding with the analyte. The MRH showed the presence of carboxyl groups on its surface. Similarly, the analyte also possess active sites capable of interacting with MRH through hydrogen bonding.

3.1. FTIR, SEM and surface area studies

Fig. S2 represents FTIR spectrums of rice husk before and after modification with NaOH.

The peaks at 1,737.8; 1,435.6 and 1,365.4 cm^{-1} were associated to C=O stretching, OH bending of the adsorbed H_2O and aliphatic C-H bending, respectively [58]. The peaks at 1,217.0; 1,365.4; 1,737.8 and 1,027.4 cm^{-1} were because of carboxyl group on MRH in the range of reported peaks at 1,208–1,230; 1,367-1,371; 1,740 and 1,029 cm^{-1} for carboxyl group [59,60]. The peak at 3,400-3,200 cm^{-1} was due to the surface O-H stretching, whereas aliphatic C–H stretching had a broad band at 2,921–2,851 cm^{-1}. The lack of band related to non-conjugated carbonyl functional groups in the MRH spectrum suggested hydrolyses of carbonyl groups during NaOH treatment. Except, the band at 1,074.0 cm^{-1} coincided to anti-symmetric stretching vibration of Si-O, while at 476.2 cm^{-1} exhibited the bending vibration of Si-O-Si bond [59,61,62].

The CR's adsorption onto MRH caused slight shifts in the position as well as intensities of bands as shown in Fig. S3. The intensities declined indicating the involvement of these groups in CR's adsorption from an aqueous solution onto MRH. The presence of carboxyl groups are most probably the mechanistic sites being capable of forming hydrogen bonds with CR leading to its adsorption on the surface of MRH.

Fig. S4 denotes MRH morphology before and after modification with NaOH, studied by using scanning electron microscopy (SEM). It was noted that the surface of RH was rough before treatment with NaOH, however after treatment, it turned smoother (Fig. S4). The chemical treatment helps to remove the surface layers of the tissues of rice husk making them smoother. Moreover, as mentioned in previous studies too, the base treatment caused an increase in surface area of rice husk as compared to raw biomass. An approximately two fold increase was observed. The surface area of raw rice husk was found to be 1.03 m^{2}g^{-1} which increased to 2.5 m^{2}g^{-1} after treatment. Similarly porosity also increased from 70% to 77% respectively.

3.2. Effect of operational factors on CR adsorption onto MRH

The effect of operational factors on the CR removal from an aqueous solution by using MRH in terms of adsorption capacity and removal efficiency was studied as described below:

3.2.1. Effect of contact time

The effect of contact time on the percentage removal and adsorption capacity of CR was illustrated and attained results are represented in Fig. 1a. Both the percentage removal of CR from an aqueous solution and adsorption capacity were found to be enhanced with contact time which was similar to our previous work [53]. From Fig. 1a it was noted that the percentage removal of CR and adsorption capacity were increased from 42% to 91% and 0.33 to 0.72 mg/g with contact time, respectively. Adsorption of CR from an aqueous solution onto MRH is represented in Fig. S5. It was seen that CR adsorption from an aqueous solution onto MRH was fast at initial stage because of existence of several empty sites on the surface of adsorbent. With the progression of adsorption process, the available sites onto surface of adsorbent were decreased leading to decline to CR adsorption onto MRH from an aqueous solution. Moreover, the fast at the beginning of the adsorption process attributed to the boundary film diffusion onto the surface of the adsorbent. Next, a slower rate of removal was obtained and attributed to the pore diffusion of CR molecules into the internal pores of the adsorbent. After 210 min, no major changes in the removal efficiency and adsorption capacity were noted and very few particles of CR were found to occupy space. The maximum CR adsorption from an aqueous solution onto MRH was attained after 210 min. It was optimum time for CR adsorption from an aqueous solution onto MRH which was used in further experiment.

3.2.2. Effect of MRH dosage

The effect of mass of adsorbent on the percentage removal of CR from an aqueous solution and adsorption capacity was also investigated at room temperature. Fig. 1b represents the effect of mass of adsorbent onto the percentage removal of CR and adsorption capacity. Results showed that the CR percentage removal was increased from 40% to 91%. It is associated with an increase in number of available active sites for CR adsorption due to increase in mass of MRH against constant concentration of CR ions. Contrary, the value of adsorption capacity declined from 1.73 to 0.72 mg/g the with increasing mass of MRH from 0.10 to 0.50 g. It was due to the limited initial concentration of CR in an aqueous solution and the inverse relationship between the adsorption capacity and the mass of the adsorbent [53,63]. More than 90% removal of CR was achieved using 0.5 g of the adsorbent and hence this dose was selected for the rest of the experiments.

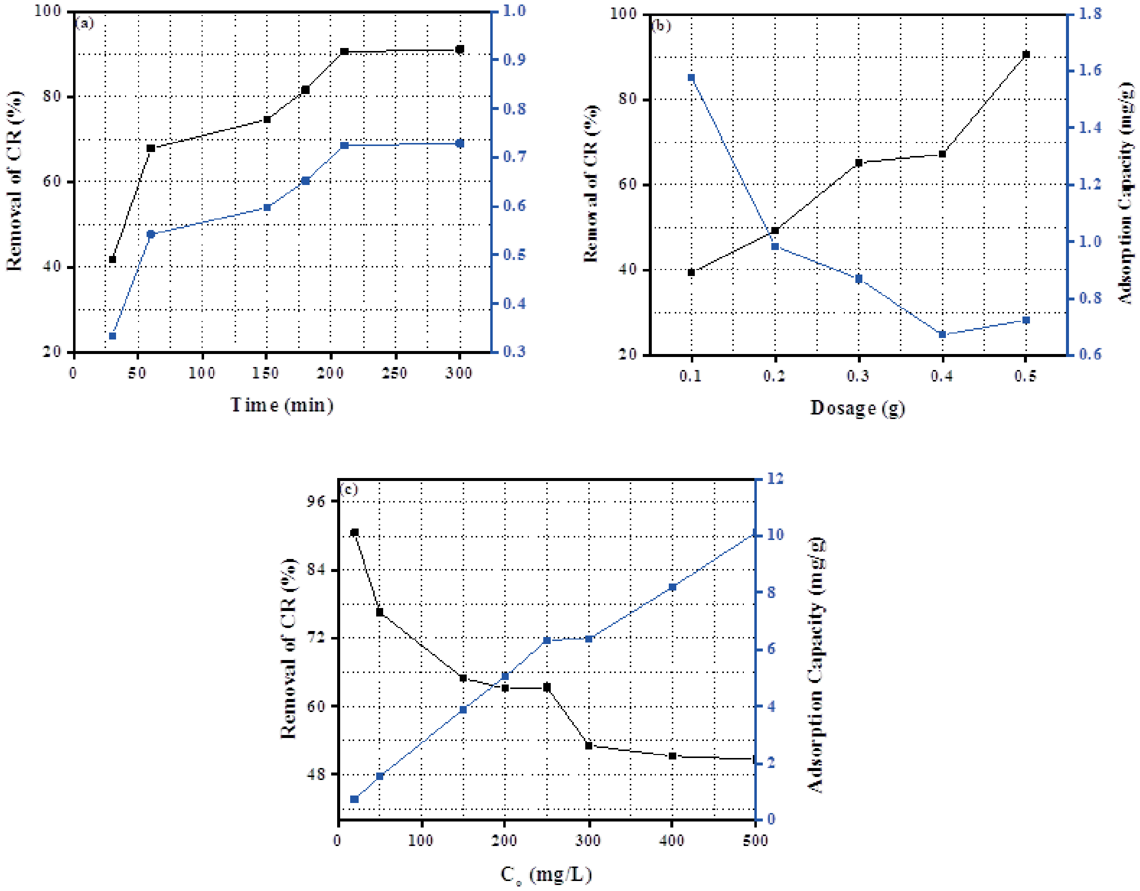

Fig. 1. (a) Effect of contact time, (b) dosage, and (c) initial concentration of CR in an aqueous solution on the percentage removal of CR from an aqueous solution and adsorption capacity.

3.2.3. Effect of initial concentration

The effect of initial concentration of an aqueous solution on the CR percentage removal and adsorption capacity was also explored and results are depicted in Fig. 1c. As represented in Fig. 1c, the removal of CR was found to be decreased while adsorption capacity increased with increase in initial concentration of CR in an aqueous solution at room temperature which is similar to our previous work [53]. The CR removal was declined from 91% to 51% while adsorption capacity increased from 0.72 to 10 mg/g with increase in CR initial concentration from 20 to 500 mg/L (Fig. 1c). The decline in the removal efficiency with increasing the initial concentration of CR ions is ascribed to the extra CR ions suspended in the solution against a constant weight of the adsorbent. A fixed amount of adsorbent can attain a certain amount of a pollutant and further increasing the concentration of the pollutant will increase the left over concentration in the effluent solution and hence decreased removal efficiency. On the other hand, the enhancement in adsorption capacity was due to increase in transportation of its molecules from an aqueous solution to MRH surface with increase in initial concentration of CR in an aqueous solution.

3.2.4. Effect of temperature

Fig. 2a indicates the effect of temperature on the CR percentage removal from an aqueous solution and adsorption capacity. Results represented that both the CR percentage removal and adsorption capacity decreased with increase in temperature from 298 to 333 K. The CR removal was decreased from 91% to 53% and adsorption capacity from 0.72 to 0.43 mg/g with increase in temperature. The decrease in the removal efficiency and adsorption capacity might be attributed to the fact that: increasing the temperature will increase the mobility of CR ion at the surface of the adsorbent allowing the CR particles to escape from the adsorption sites and hence decreased removal efficiency was found. These results implying that CR adsorption from an aqueous solution onto MRH was an exothermic process.

3.2.5. Effect of pH

It is crucial to investigate the influence of pH on adsorption process. The pH has significant effect on the surface polarity of the adsorbents, ionic mobility and degree of ionization of the pollutants [64]. The change in CR percentage removal and adsorption capacity with pH is represented in Fig. 2b. From the attained results, it was observed that percentage removal of CR was 91% and adsorption capacity 0.72 mg/g at pH 6. From this, it was noted that active sites and polarity of MRH congested at higher concentration of OH^- or H^+. Therefore, CR adsorption declines at higher or lower value of pH. The ZPC of the MRH was investigated in our previous research and found to be 3.9 [65]. The effect of pH can be explained as follows, at $pH < 3.9$, the adsorbent is positively charged and the anionic dye CR is getting adsorbed due to the electrostatic interactions leading to a removal efficiency of more than 55%. At pH 5, the adsorbent is negatively charged and the anionic dye is getting adsorbed by ion exchange mechanism with OH^- groups. The FTIR results found to support the contribution of OH^- groups in the removal process. Interestingly, it can be said that the ion exchange mechanism has a greater contribution in the removal process than the electrostatic interactions leading to a removal efficiency of more than 90% at pH 5. However, further increasing the solution pH to highly acidic conditions (i.e., $pH \geq 6.9$), the removal efficiency and adsorption capacity found to decrease. These results might be explained as follows: increasing the concentration of OH^- in the bulk solution prevent the suspended CR ions from getting exchange with the OH^- ions on the surface of the adsorbent and hence decreased removal efficiency. However, the removal efficiency at pH 12 was still more than 65% which is higher than the removal at pH 2 (60%) which in turn again support our finding that ion exchange mechanism can contribute toward the removal of CR by MRH more than the electrostatic interactions.

3.3. Adsorption isotherms

Several adsorption isotherms including Langmuir, Freundlich, Temkin and Dubinin–Radushkevich (D–R)

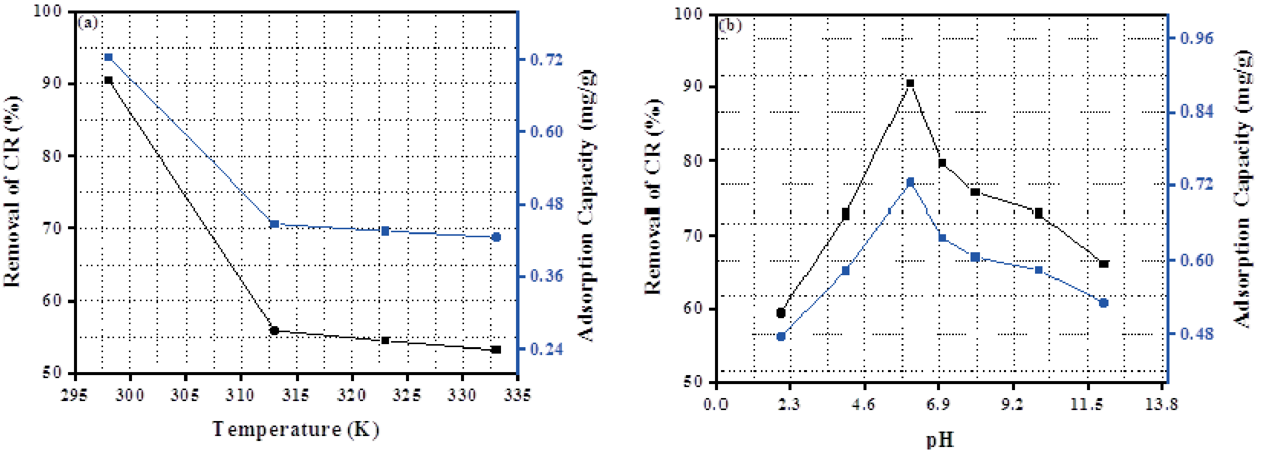

Fig. 2. (a) Effect of temperature and (b) pH on the percentage removal of CR from an aqueous solution and adsorption capacity.

were used to explain CR adsorption from an aqueous solution onto MRH. The adsorption isotherm of C_e vs. q_e for CR adsorption onto MRH is shown in Fig. 3. The adsorption capacity was increasing with the equilibrium concentration in the investigated range of CR concentration. The experimental data were subjected to linearized fitting of the isotherm models and the obtained plots are presented in Fig. 4a–d. The plot of Langmuir isotherm is represented in Fig. 4a and the values of its measured factors are given in Table 2. The determined coefficient (R^2 = 0.865) value denoted that CR adsorption onto MRH fitted to Langmuir isotherm. The determined value of R_L (0.14–0.80) showed that CR adsorption from an aqueous solution was favorable process. For CR adsorption onto MRH, the plot for Freundlich isotherm is shown in Fig. 4b and the calculated value of its parameters are given in Table 2. The determined coefficient value (R^2 = 0.990) represented that CR adsorption from an aqueous solution onto MRH fitted well to Freundlich isotherm. The values of Freundlich constant 'n' ranges from 2–10 indicating good adsorption, 1–2 moderate adsorption and less than one denoted poor adsorption [66,67]. Fig. 4c shows the plot of Temkin isotherm for CR adsorption and the measured values of b_T and A_T are given Table 2. The determined coefficient value (R^2 = 0.823) was lower than Freundlich isotherm denoting that CR adsorption from an aqueous solution onto MRH was not fitted to Temkin isotherm. Fig. 4d represents the plot of D-R isotherm for CR adsorption. The values of D-R constant (C_m) and β were determined from intercept and slope respectively and are given in Table 2. The determined value of

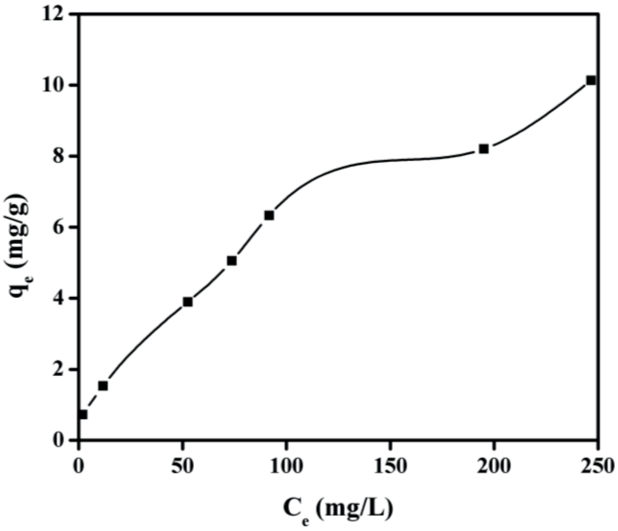

Fig. 3. Adsorption isotherm of CR adsorption onto MRH.

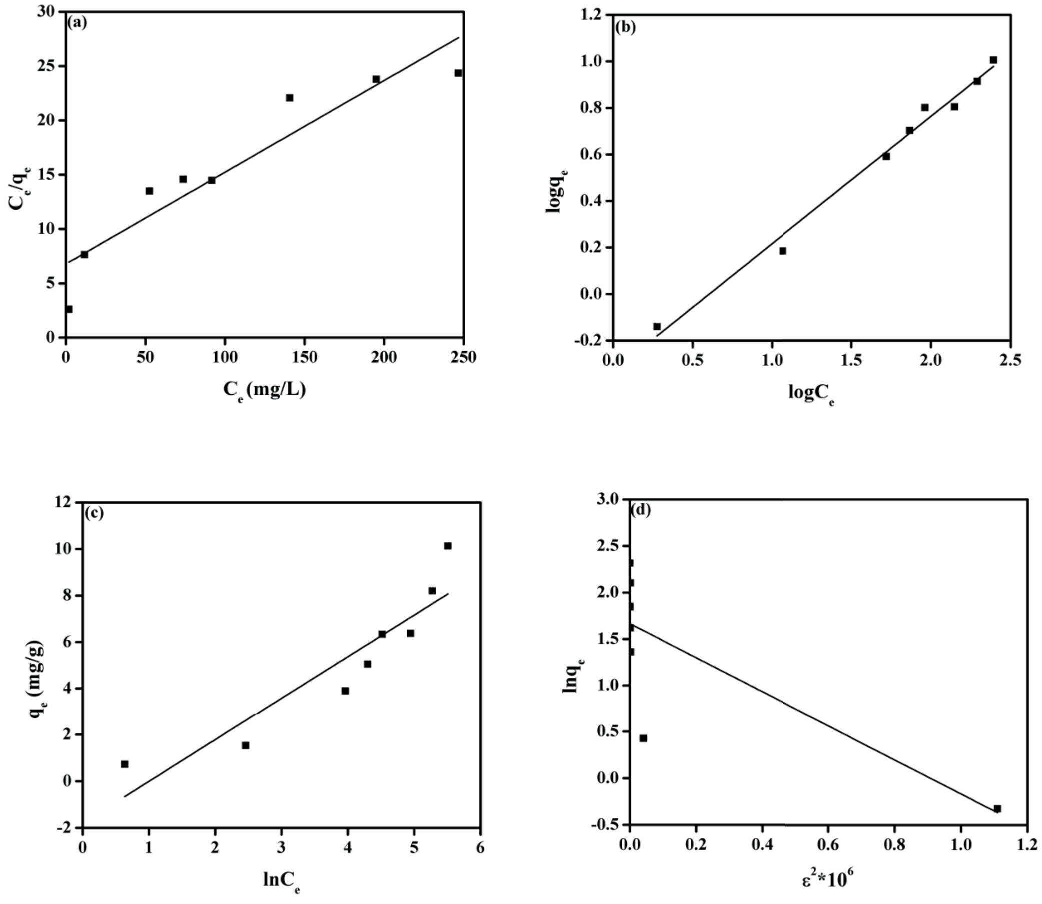

Fig. 4. (a) Langmuir isotherm, (b) Freundlich isotherm, (c) Temkin isotherm, and (d) Dubinin–Radushkevich (D-R) isotherm for CR adsorption from an aqueous solution onto MRH.

Table 2
Measured isotherms parameters for CR adsorption onto MRH from an aqueous solution

Adsorption isotherm models	Calculated parameters	
Langmuir isotherm	Q_m	11.84
	$K_L \times 10^{-2}$	1.24
	R_L	0.14–0.80
	R^2	0.865
Freundlich isotherm	N	1.83
	K_f	0.47
	R^2	0.990
Temkin isotherm	b_T	1383
	A_T	0.368
	R^2	0.823
D-R isotherm	B	1.829
	C_m	5.28
	R^2	0.562
	E	0.524

Q_m: mg/g; K_L: L/mol; K_f: (mg/g)(L/mg)$^{1/n}$; C_m: mg/g; β: mol²/J²; E: kJ/mol.

mean adsorption energy (E) for CR adsorption onto MRH was 0.524 kJ/mol. It denoted that CR adsorption from an aqueous solution onto MRH was physical adsorption process [49,55].

3.4. Adsorption kinetics

Adsorption kinetics for CR adsorption from an aqueous solution onto MRH was investigated by applying several models including pseudo-first-order model, pseudo-second-order model, Elovich model, modified Freundlich equation and Bangham equation. The pseudo-first-order model for CR adsorption from an aqueous solution onto MRH is denoted in Fig. 5a and the measured values of its parameters (k_1 and q_e) are given in Table 3. The determined coefficient (R^2) value for it was 0.815. Moreover, there was a big difference between calculated adsorption capacity values ($q_{e,\text{cal}}$ = 1.10 mg/g) and experimental adsorption capacity ($q_{e,\text{exp}}$ = 0.72 mg/g). It represented that the rate process can't be explained by pseudo-first-order model. Fig. 5b depicts the pseudo-second-order model plot for CR adsorption and the calculated values of its factors are given in Table 3. The claculated value of

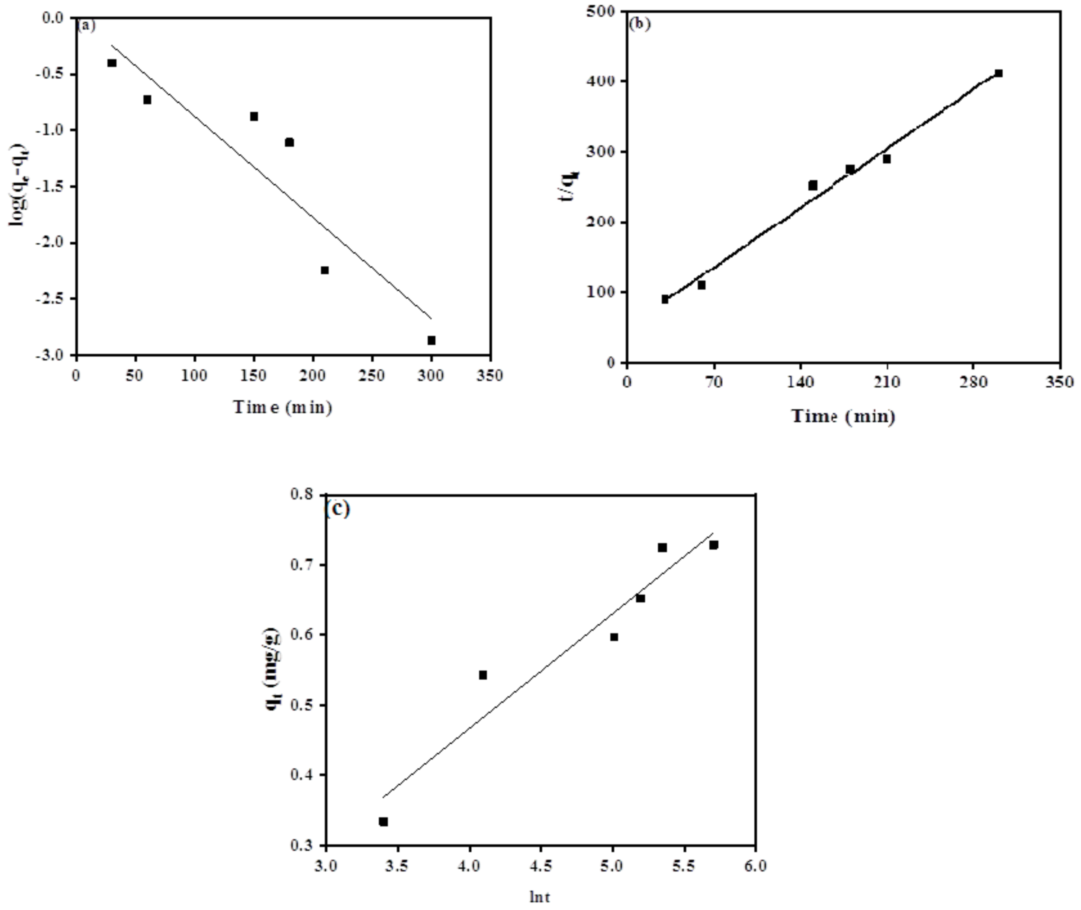

Fig. 5. (a) Pseudo-first-order model, (b) pseudo-second-order model, and (c) Elovich model for CR adsorption from an aqueous solution onto MRH.

Table 3
Measured kinetics parameters for CR adsorption onto MRH from an aqueous solution

Kinetic models	Parameters	
Pseudo-first-order model	$q_{e(\text{exp.})}$	0.72
	$q_{e(\text{cal.})}$	1.10
	$k_1 \times 10^{-3}$	9.0
	R^2	0.815
Pseudo-second-order model	q_e	0.83
	$k_2 \times 10^{-2}$	2.83
	R^2	0.990
Elovich model	A	0.052
	B	6.11
	R^2	0.909
Modified Freundlich equation	M	3.14
	k	0.006
	R^2	0.871
Bangham equation	k_o	0.13
	A	0.32
	R^2	0.872

q_e: mg/g; k_1: min^{-1}; k_2: g/mg min; α: mg/g min; β: g/mg; k: L/g min; k_o: mL/g/L.

adsorption capacity (0.83 mg/g) was close to experimental value (0.72 mg/g). Moreover, the determined coefficient (R^2 = 0.990) value was close to unity. Therefore, CR adsorption from an aqueous solution onto MRH fitted well to pseudo-second-order model. Moreover, Elovich model's plot for CR adsorption onto MRH is shown in Fig. 5c and the calculated values of it factors (α and β) are given in Table 3. The determined coefficient (R^2 = 0.909) value was smaller than pseudo-second-order model denoting that it is not sufficient to explain CR adsorption from an aqueous solution.

Fig. 6a indicates modified Freundlich equation plot for CR from an aqueous solution onto MRH and the measured values of its parameters (m & k) are given in Table 3. From Table 3, it was seen that the determined coefficient (R^2 = 0.871) value was smaller than pseudo-second-order model. It means that it can't explain CR adsorption onto MRH. For CR adsorption, Bangham equation plot is represented in Fig. 6b and the attained values of its parameters are given in Table 3. For Bangham eaquation, the determined coefficient value (R^2 = 0.954) was smaller than pseudo-second-order model (Table 3). The double logarithmic plot did not give linear curve for CR adsorption onto MRH indicating that the diffusion of adsorbate (CR) into pores of the adsorbent (MRH) is not the only rate controlling step [51]. For CR adsorption from an aqueous solution

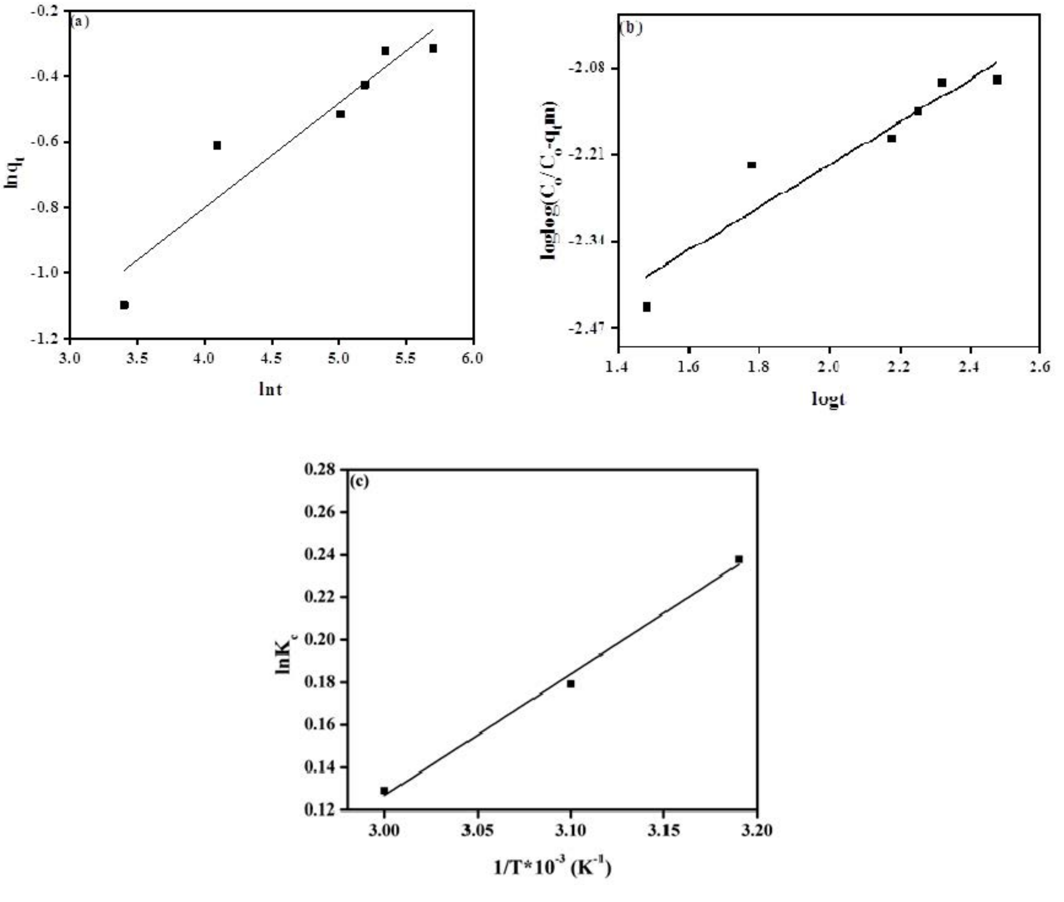

Fig. 6. (a) Modified Freundlich equation, (b) Bangham equation, and (c) the plot of $1/T$ vs. $\ln K_c$ for CR adsorption from an aqueous solution onto MRH.

Table 4
Measured thermodynamic parameters adsorption of CR onto MRH from aqueous solution

Temperature (K)	Δ*H* (kJ/mol)	Δ*S* (J/K mol)	Δ*G* (kJ/mol)
298	–4.75	–13.19	3.93
313			4.12
323			4.25
333			4.39

onto MRH, it may be that both film and pore diffusion was significant to different extent which in turn supports the results of effect of contact time (section 3.2.3).

3.5. Adsorption thermodynamics

For CR adsorption from an aqueous solution onto MRH, adsorption thermodynamics was investigated by determining change in Gibb's free (Δ*G*°), enthalpy (Δ*H*°) and entropy (Δ*S*°). Fig. 6c denotes the plot of $1/T$ vs. $\ln K_c$ for CR adsorption from an aqueous solution onto MRH and the calculated values of thermodynamic parameters are given in Table 4. It was noted that the value of change in enthalpy ($\Delta H°$ = –4.75 kJ/mol) was negative for CR adsorption from an aqueous solution representing that CR adsorption onto MRH was exothermic process [56,68,69]. The negative value of change in entropy for CR adsorption onto MRH indicated the decrease in randomness at adsorbate–adsorbent interface during CR adsorption onto MRH. Contrary, the values of Gibb's free energy (Δ*G*°) for CR adsorption from an aqueous solution onto MRH were positive. The values of Gibb's free energy increased from 3.93 to 4.39 kJ/mol with rise in temperature from 298 to 333 K. It was associated to interaction between the dyes on solid surface with non-equal competition attributed to the heterogeneity of adsorbent surface and the system gained energy from external source at high temperatures.

3.6. Comparative analysis

Congo red being a hazardous dye remained the focus of study by a number of research groups and its abatement from waste water through biomasses is highly demanding. Sharma et al., used Cornulaca monacantha stem as a biosorbent and a maximum removal of 86.5% was attained. The adsorbent possessed irregular and rough surface with low porosity and contain –O–CH_3, –OH, C=O as functional groups [70]. Similarly, Ulva lactuca has been evaluated for CR removal which is a sustainable biomass feedstock. The biomass was able to efficiently adsorb 97.9% of the dye [71]. Trametes versicolor, a type of fungus was used native as well as pretreated by Binupriya et al. and found that treated biomass showed better removal. Various experimental parameters were evaluated and a maximum removal of 98.9% was observed under acidic conditions [72].

The modified rice husk in present study presented a percentage removal of 91% at acidic pH. The chemical treatment improved the surface properties of the biosorbent, moreover, it is easily available and cost effective.

4. Conclusions

The conducted work reported the capability of chemically treated rice husk to serve an adsorbent using CR as model dye and discussed various parameters that can affect its adsorbent capacity. The chemical treatment resulted in an increase in surface area and also helped in removing the inorganic materials present on the rice husk surface. Moreover, the porosity of the biomass also increased from 70% to 77%. The batch adsorption of CR from an aqueous solution onto MRH was performed at room temperature. FTIR test confirmed CR adsorption onto MRH. The removal of CR increased with contact time, mass of adsorbent (MRH) while decline with initial concentration CR in an aqueous solution and temperature. Adsorption capacity was increased with contact time and initial concentration of CR in an aqueous solution while decrease with dosage (MRH) and temperature. The maximum adsorption capacity was found to be 0.72 mg/g. With pH, both the percentage removal of CR and adsorption capacity firstly increased and then decreased. Adsorption of CR from an aqueous solution onto MRH followed Freundlich isotherm and hence was a physiosorption process. Kinetic study represented that adsorption of CR fitted to pseudo-second-order kinetics. Moreover, adsorption of CR onto MRH was an exothermic process suggesting the adsorption phenomenon to be spontaneous in nature. Hence MRH could be used for CR adsorption at room temperature from an aqueous solution.

Acknowledgement

This work was funded by the University of Sharjah (UoS) grant number UoS-130508, PI: A. Shanableh.

References

[1] I. Ali, A.A. Basheer, X.Y. Mbianda, A. Burakov, E. Galunin, I. Burakova, E. Mkrtchyan, A. Tkachev, V. Grachev, Graphene based adsorbents for remediation of noxious pollutants from wastewater, Environ. Int., 127 (2019) 160–180.

[2] A.A. Basheer, New generation nano-adsorbents for the removal of emerging contaminants in water, J. Mol. Liq., 261 (2018) 583–593.

[3] I. Ali, Z.A. Alothman, A. Al-Warthan, Sorption, kinetics and thermodynamics studies of atrazine herbicide removal from water using iron nano-composite material, Int. J. Environ. Sci. Technol., 13 (2016) 733–742.

[4] R. Nodehi, H. Shayesteh, A.R. Kelishami, Enhanced adsorption of congo red using cationic surfactant functionalized zeolite particles, Microchem. J., 153 (2020) 104281.

[5] J. Wang, S. Zheng, Y. Shao, J. Liu, Z. Xu, D. Zhu, Amino-functionalized Fe_3O_4@SiO_2 core–shell magnetic nanomaterial as a novel adsorbent for aqueous heavy metals removal, J. Colloid Interface Sci., 349 (2010) 293–299.

[6] I. Ali, O.M.L. Alharbi, Z.A. Alothman, A.Y. Badjah, A. Alwarthan, A.A. Basheer, Artificial neural network modelling of amido black dye sorption on iron composite nano material: kinetics and thermodynamics studies, J. Mol. Liq., 250 (2018) 1–8.

[7] M. Shaban, M.I. Sayed, M.G. Shahien, M.R. Abukhadra, Z.M. Ahmed, Adsorption behavior of inorganic- and organic-modified kaolinite for Congo red dye from water, kinetic modeling, and equilibrium studies, J. Sol-Gel Sci. Technol., 87 (2018) 427–441.

[8] A.Z.M. Badruddoza, A.S.H. Tay, P.Y. Tan, K. Hidajat, M.S. Uddin, Carboxymethyl-β-cyclodextrin conjugated

magnetic nanoparticles as nano-adsorbents for removal of copper ions: synthesis and adsorption studies, J. Hazard. Mater., 185 (2011) 1177–1186.

[9] H. Shayesteh, A. Ashrafi, A. Rahbar-Kelishami, Evaluation of Fe_3O_4@MnO_2 core-shell magnetic nanoparticles as an adsorbent for decolorization of methylene blue dye in contaminated water: synthesis and characterization, kinetic, equilibrium, and thermodynamic studies, J. Mol. Struct., 1149 (2017) 199–205.

[10] R. Jothirani, P.S. Kumar, A. Saravanan, A.S. Narayan, A. Dutta, Ultrasonic modified corn pith for the sequestration of dye from aqueous solution, J. Ind. Eng. Chem., 39 (2016) 162–175.

[11] A. Ullah, M. Zahoor, W.U. Din, M. Muhammad, F.A. Khan, A. Sohail, R. Ullah, E.A. Ali, H. Murthy, Removal of methylene blue from aqueous solution using black tea wastes: used as efficient adsorbent, Adsorpt. Sci. Technol., 2022 (2022).

[12] Y.-M. Hao, C. Man, Z.-B. Hu, Effective removal of Cu(II) ions from aqueous solution by amino-functionalized magnetic nanoparticles, J. Hazard. Mater., 184 (2010) 392–399.

[13] I.M. Banat, P. Nigam, D. Singh, R. Marchant, Microbial decolorization of textile-dyecontaining effluents: a review, Bioresour. Technol., 58 (1996) 217–227.

[14] B.M. Mohamed Amine Zenasni, A. Merlin, B. George, Adsorption of Congo red from aqueous solution using CTAB-kaolin from bechar Algeria, J. Surf. Eng. Mater. Adv. Technol., 4 (2014) 332–341.

[15] G. Li, B. Liu, L. Bai, Z. Shi, X. Tang, J. Wang, H. Liang, Y. Zhang, B. Van der Bruggen, Improving the performance of loose nanofiltration membranes by poly-dopamine/zwitterionic polymer coating with hydroxyl radical activation, Sep. Purif. Technol., 238 (2020) 116412.

[16] J. Yu, D. Zhang, W. Ren, B. Liu, Transport of Enterococcus faecalis in granular activated carbon column: potential energy, migration, and release, Colloids Surf., B, 183 (2019) 110415.

[17] A. Demirbas, Agricultural based activated carbons for the removal of dyes from aqueous solutions: a review, J. Hazard. Mater., 167 (2009) 1–9.

[18] S.M. Ghoreishi, R. Haghighi, Chemical catalytic reaction and biological oxidation for treatment of non-biodegradable textile effluent, Chem. Eng. J., 95 (2003) 163–169.

[19] J. Yu, A. Zou, W. He, B. Liu, Adsorption of mixed dye system with cetyltrimethylammonium bromide modified sepiolite: characterization, performance, kinetics and thermodynamics, Water, 12 (2020) 981.

[20] S. Shao, W. Fu, X. Li, D. Shi, Y. Jiang, J. Li, T. Gong, X. Li, Membrane fouling by the aggregations formed from oppositely charged organic foulants, Water Res., 159 (2019) 95–101.

[21] V.K. Garg, R. Gupta, A. Bala Yadav, R. Kumar, Dye removal from aqueous solution by adsorption on treated sawdust, Bioresour. Technol., 89 (2003) 121–124.

[22] S. Babel, T.A. Kurniawan, Low-cost adsorbents for heavy metals uptake from contaminated water: a review, J. Hazard. Mater., 97 (2003) 219–243.

[23] I. Ali, M. Asim, T.A. Khan, Low cost adsorbents for the removal of organic pollutants from wastewater, J. Environ. Manage., 113 (2012) 170–183.

[24] Ihsanullah, A. Abbas, A.M. Al-Amer, T. Laoui, M.J. Al-Marri, M.S. Nasser, M. Khraisheh, M.A. Atieh, Heavy metal removal from aqueous solution by advanced carbon nanotubes: critical review of adsorption applications, Sep. Purif. Technol., 157 (2016) 141–161.

[25] J. Song, T. Xu, M.L. Gordin, P. Zhu, D. Lv, Y.-B. Jiang, Y. Chen, Y. Duan, D. Wang, Nitrogen-doped mesoporous carbon promoted chemical adsorption of sulfur and fabrication of high-areal-capacity sulfur cathode with exceptional cycling stability for lithium-sulfur batteries, Adv. Funct. Mater., 24 (2014) 1243–1250.

[26] M. Grassi, L. Rizzo, A. Farina, Endocrine disruptors compounds, pharmaceuticals and personal care products in urban wastewater: implications for agricultural reuse and their removal by adsorption process, Environ. Sci. Pollut. Res., 20 (2013) 3616–3628.

[27] M.J. Tillotson, P.M. Brett, R.A. Bennett, R. Grau-Crespo, Adsorption of organic molecules at the TiO_2(110) surface: the effect of van der Waals interactions, Surf. Sci., 632 (2015) 142–153.

[28] R.-k. Xu, S.-c. Xiao, J.-h. Yuan, A.-z. Zhao, Adsorption of methyl violet from aqueous solutions by the biochars derived from crop residues, Bioresour. Technol., 102 (2011) 10293–10298.

[29] A. Çelekli, S.S. Birecikligil, F. Geyik, H. Bozkurt, Prediction of removal efficiency of Lanaset Red G on walnut husk using artificial neural network model, Bioresour. Technol., 103 (2012) 64–70.

[30] Y. Yang, D. Jin, G. Wang, D. Liu, X. Jia, Y. Zhao, Biosorption of Acid Blue 25 by unmodified and CPC-modified biomass of Penicillium YW01: kinetic study, equilibrium isotherm and FTIR analysis, Colloids Surf., B, 88 (2011) 521–526.

[31] H. Zhu, R. Jiang, Y.-Q. Fu, J.-H. Jiang, L. Xiao, G.-M. Zeng, Preparation, characterization and dye adsorption properties of γ-Fe_2O_3/SiO_2/chitosan composite, Appl. Surf. Sci., 258 (2011) 1337–1344.

[32] T. Farías, L.C. de Ménorval, J. Zajac, A. Rivera, Benzalkonium chloride and sulfamethoxazole adsorption onto natural clinoptilolite: effect of time, ionic strength, pH and temperature, J. Colloid Interface Sci., 363 (2011) 465–475.

[33] M. Ghaedi, H. Hossainian, M. Montazerozohori, A. Shokrollahi, F. Shojaipour, M. Soylak, M. Purkait, A novel acorn based adsorbent for the removal of brilliant green, Desalination, 281 (2011) 226–233.

[34] X.-Y. Huang, H.-T. Bu, G.-B. Jiang, M.-H. Zeng, Cross-linked succinyl chitosan as an adsorbent for the removal of Methylene Blue from aqueous solution, Int. J. Biol. Macromol., 49 (2011) 643–651.

[35] Y. Feng, F. Yang, Y. Wang, L. Ma, Y. Wu, P.G. Kerr, L. Yang, Basic dye adsorption onto an agro-based waste material–Sesame hull (*Sesamum indicum* L.), Bioresour. Technol., 102 (2011) 10280–10285.

[36] M. Akgül, A. Karabakan, Promoted dye adsorption performance over desilicated natural zeolite, Microporous Mesoporous Mater., 145 (2011) 157–164.

[37] T. Kan, X. Jiang, L. Zhou, M. Yang, M. Duan, P. Liu, X. Jiang, Removal of methyl orange from aqueous solutions using a bentonite modified with a new gemini surfactant, Appl. Clay Sci., 54 (2011) 184–187.

[38] A.Y. Dursun, O. Tepe, Removal of Chemazol Reactive Red 195 from aqueous solution by dehydrated beet pulp carbon, J. Hazard. Mater., 194 (2011) 303–311.

[39] B. Balci, Basic textile dye adsorption from aqueous solution and synthetic dye bath wastewater by modified eucalyptus barks, Fresenius Environ. Bull., 25 (2016) 6124–6131.

[40] A. Xue, S. Zhou, Y. Zhao, X. Lu, P. Han, Effective NH_2-grafting on attapulgite surfaces for adsorption of reactive dyes, J. Hazard. Mater., 194 (2011) 7–14.

[41] J.d.J. da Silveira Neta, G.C. Moreira, C.J. da Silva, C. Reis, E.L. Reis, Use of polyurethane foams for the removal of the Direct Red 80 and Reactive Blue 21 dyes in aqueous medium, Desalination, 281 (2011) 55–60.

[42] K. Elass, A. Laachach, A. Alaoui, M. Azzi, Removal of methyl violet from aqueous solution using a stevensite-rich clay from Morocco, Appl. Clay Sci., 54 (2011) 90–96.

[43] G. Lv, Z. Li, W.-T. Jiang, P.-H. Chang, J.-S. Jean, K.-H. Lin, Mechanism of acridine orange removal from water by low-charge swelling clays, Chem. Eng. J., 174 (2011) 603–611.

[44] H. Chen, J. Zhao, A. Zhong, Y. Jin, Removal capacity and adsorption mechanism of heat-treated palygorskite clay for methylene blue, Chem. Eng. J., 174 (2011) 143–150.

[45] R. Gnanasekaran, B. Dhandapani, A. Saravanan, Biosorption of methylene blue dye by chemically modified *Aspergillus japonicus* MG183814: kinetics, thermodynamic and equilibrium studies, Desal. Water Treat., 122 (2018) 132–145.

[46] Y. Diquarternasi, Removal of basic blue 3 and reactive orange 16 by adsorption onto q uartenized sugar cane bagasse, Malaysian J. Anal. Sci., 13 (2009) 185–193.

[47] A.G. Despina, Why reuse spent adsorbents? The latest challenges and limitations, Sci. Total Environ., 822 (2022) pp. 153612–152022 v. 153822.

[48] S. Zafar, M.I. Khan, A. Shanableh, S. Ahmad, S. Manzoor, S. Shahida, P. Prapamonthon, S. Mubeen, A. Rehman,

Adsorption of silver, thorium and nickel ions from aqueous solution onto rice husk, Desal. Water Treat., 236 (2021) 108–122.

[49] M.I. Khan, S. Zafar, M.A. Khan, F. Mumtaz, P. Prapamonthon, A.R. Buzdar, Bougainvillea glabra leaves for adsorption of congo red from wastewater, Fresenius Environ. Bull., 27 (2018) 1456–1465.

[50] M.I. Khan, S. Zafar, M.A. Khan, A.R. Buzdar, P. Prapamonthon, Adsorption kinetic, equilibrium and thermodynamic study for the removal of Congo Red from aqueous solution, Desal. Water Treat., 98 (2017) 294–305.

[51] S. Zafar, M.I. Khan, H. Rehman, J. Fernandez-Garcia, S. Shahida, P. Prapamonthon, M. Khraisheh, A. Rehman, H.B. Ahmad, M.L. Mirza, N. Khalid, M.H. Lashari, Kinetic, equilibrium, and thermodynamic studies for adsorptive removal of cobalt ions by rice husk from aqueous solution, Desal. Water Treat., 204 (2020) 285–296.

[52] S. Zafar, M.I. Khan, M. Khraisheh, M.H. Lashari, S. Shahida, M.F. Azhar, P. Prapamonthon, M.L. Mirza, N. Khalid, Kinetic, equilibrium and thermodynamic studies for adsorption of nickel ions onto husk of *Oryza sativa*, Desal. Water Treat., 167 (2019) 277–290.

[53] M.I. Khan, A. Shanableh, J. Fernandez, M.H. Lashari, S. Shahida, S. Manzoor, S. Zafar, A. ur Rehman, N. Elboughdiri, Synthesis of DMEA-grafted anion exchange membrane for adsorptive discharge of methyl orange from wastewaters, Membranes, 11 (2021) 166.

[54] M.I. Khan, J. Su, L. Guo, Development of triethanolamine functionalized-anion exchange membrane for adsorptive removal of methyl orange from aqueous solution, Desal. Water Treat., 209 (2021) 342–352.

[55] M.I. Khan, S. Zafar, A.R. Buzdar, M.F. Azhar, W. Hassan, A. Aziz, Use of citrus sinensis leaves as a bioadsorbent for removal of congo red dye from aqueous solution, Fresenius Environ. Bull., 27 (2018) 4679–4688.

[56] M.I. Khan, S. Akhtar, S. Zafar, A. Shaheen, M.A. Khan, R. Luque, Removal of congo red from aqueous solution by anion exchange membrane (EBTAC): adsorption kinetics and themodynamics, Materials, 8 (2015) 4147–4161.

[57] M.A. Khan, M.I. Khan, S. Zafar Removal of different anionic dyes from aqueous solution by anion exchange membrane, Membr. Water Treat., 8 (2017) 259–277.

[58] S.K. Kazy, S. D'Souza, P. Sar, Uranium and thorium sequestration by a *Pseudomonas* sp.: mechanism and chemical characterization, J. Hazard. Mater., 163 (2009) 65–72.

[59] V.C. Srivastaa, I.D. Mall, I.M. Mishra, Characterization of mesoporous rice husk ash (RHA) and adsorption kinetics of metal ions from aqueous solution onto RHA, J. Hazard. Mater., 134 (2006) 257.

[60] S.K. Kazy, K. Sar, P. Sen, A.K. Singh, S.F. D'Souza, Extracellular polysaccha-rides of a copper sensitive and a copper resistant *Pseudomonas aeruginosa* stain: synthesis, chemical nature and copper binding, World J. Microbiol. Biotechnol., 18 (2002) 583.

[61] X. Ying-Mei, H.D.-M. Qi. Ji, W. Dong-Mei, C. Hui-Ying, G. Jun, Q.-M.Z., Preparation of amorphous silica from oil shale residue and surface modification by silane coupling agent, Oil Shale, 27 (2010) 37–46.

[62] L. Ludueña, D. Fasce, V.A. Alvarez, P.M. Stefani, Nanocellulose from rice husk following alkaline treatment to remove silica, BioResources, 6 (2011) 1440–1453.

[63] Y.-S. Ho, Second-order kinetic model for the sorption of cadmium onto tree fern: a comparison of linear and non-linear methods, Water Res., 40 (2006) 119–125.

[64] Y. Ren, X. Wei, M. Zhang, Adsorption character for removal Cu(II) by magnetic Cu(II) ion imprinted composite adsorbent, J. Hazard. Mater., 158 (2008) 14–22.

[65] I.W. Almanassra, M.I. Khan, M.A. Atieh, A. Shanableh, Adsorption of lead ions from aqueous solution onto NaOH-modified rice husk, Desal. Water Treat., (2022), doi: 10.5004/dwt.2022.28568.

[66] M.I. Khan, A. Shanableh, N. Nasir, S. Shahida, Adsorptive removal of methyl orange from wastewaters by the commercial anion exchange membrane EPTAC, Desal. Water Treat., 234 (2021) 245–254.

[67] M.I. Khan, M.H. Lashari, M. Khraisheh, S. Shahida, S. Zafar, P. Prapamonthon, A. Rehman, S. Anjum, N. Akhtar, F. Hanif, Adsorption kinetic, equilibrium and thermodynamic studies of Eosin-B onto anion exchange membrane, Desal. Water Treat., 155 (2019) 84–93.

[68] M.A. Khan, M.I. Khan, S. Zafar, Removal of different anionic dyes from aqueous solution by anion exchange membrane, Membr. Water Treat., 8 (2016) 259–277.

[69] I.W. Almanassra, G. McKay, V. Kochkodan, M. Ali Atieh, T. Al-Ansari, A state of the art review on phosphate removal from water by biochars, Chem. Eng. J., 409 (2021) 128211.

[70] A. Sharma, Z.M. Siddiqui, S. Dhar, P. Mehta, D. Pathania, Adsorptive removal of congo red dye (CR) from aqueous solution by *Cornulaca monacantha* stem and biomass-based activated carbon: isotherm, kinetics and thermodynamics, Sep. Sci. Technol., 54 (2019) 916–929.

[71] N. El-Ahmady El-Naggar, N.H. Rabei, S.E. El-Malkey, Eco-friendly approach for biosorption of Pb^{2+} and carcinogenic Congo red dye from binary solution onto sustainable *Ulva lactuca* biomass, Sci. Rep., 10 (2020) 1–22.

[72] A.R. Binupriya, M. Sathishkumar, D. Kavitha, K. Swaminathan, S.E. Yun, S.P. Mun, Experimental and isothermal studies on sorption of Congo red by modified mycelial biomass of wood-rotting fungus, CLEAN–Soil, Air, Water, 35 (2007) 143–150.

Supporting information

S1. Adsorption of CR from an aqueous solution onto MRH

Initially, the standard solution of CR was prepared by dissolving it into distilled water. The determined quantity of MRH was shaked at agitation speed of 140 rmp into 20 mL of CR aqueous solution. The determined mass of MRH (0.50 g) was shaked into 20 mL of CR aqueous solution with initial concentration of 20 mg/L for different time intervals including 30, 60, 90, 120, 150, 180, 210, 240, 270, and 300 min to find out optimum contact time. The optimized mass of MRH was determined by using varying masses of the MRH from 0.10 to 0.50 g into 20 mL of CR aqueous solution with initial concentration of 20 mg/L of CR in an aqueous solution for 210 min. The measured amount of MRH (0.50 g) was shaked for 210 min into 20 mL of CR in an aqueous solution with initial concentration of 20, 50, 100, 150, 200, 250, 300, 400 and 500 mg/L to investigate adsorption isotherms. To investigate adsorption thermodynamics, the calculated mass of MRH (0.50 g) was shaked into 20 mL of CR aqueous solution with initial concentration of 20 mg/L at 298, 313, 323 and 333 K for at speed 140 rmp 210 min. The effect of pH on CR adsorption was studied by shaking measured mass of MRH (0.50 g) into 20 mL of CR aqueous solution with initial concentration of 20 mg/L at stirring speed of 140 rmp for 210 min at room temperature. The CR concentration was measured by recording absorbance of the supernatant at wavelength (λ_{max}) of 490 nm by using UV/VIS spectrophotometer (UV-2550, SHIMADZU). The calibration curve was used to determine concentration of CR in an aqueous solution. The removal of CR from an aqueous solution and adsorption capacity was recorded by using below equations:

$$\text{Removal} = \frac{C_o - C_t}{C_o} \times 100 \tag{S1}$$

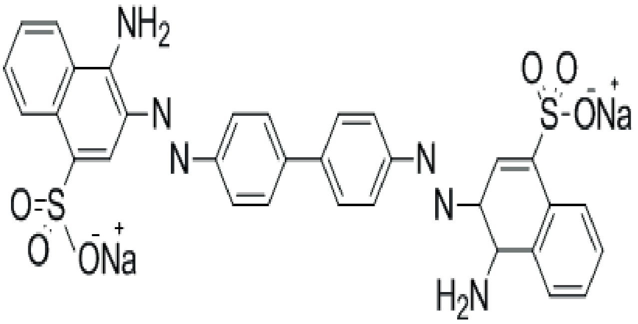

Fig. S1. Chemical structure of Congo red (CR) dye.

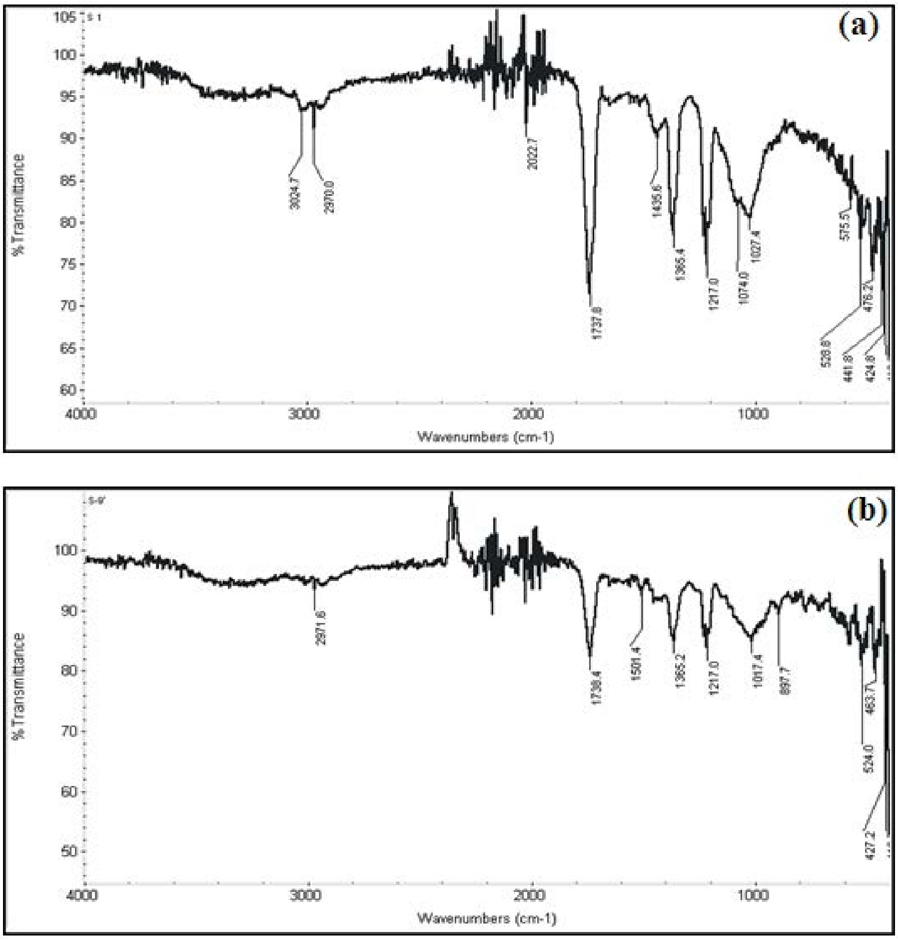

Fig. S2. FTIR spectrums of (a) rice husk (RH) and (b) modified rice husk (MRH).

$$q_t = \frac{C_o - C_t}{W} \times V \tag{S2}$$

where C_o and C_t denote CR concentration at initial stage and at time t respectively. Similarly V and W indicate volume of CR aqueous solution and mass of MRH respectively.

S2. Adsorption isotherms

S2.1. Langmuir isotherm

It is based on the maximum adsorption corresponds to saturated monolayer of liquid molecules on the solid surface. It is shown as [S1,S2]:

$$\frac{C_e}{q_e} = \frac{1}{K_L Q_m} + \frac{C_e}{Q_m} \tag{S3}$$

where K_L is Langmuir constant (L/mg) and Q_m is Langmuir monolayers adsorption capacity (mg/g), C_e is supernatant concentration at equilibrium state of the system (mg/L), and q_e is the amount of dye adsorbed at equilibrium state of system (mg/g). The essential characteristics of Langmuir isotherm can be denoted in term of dimensionless constant separation factor R_L that is shown as [S3].

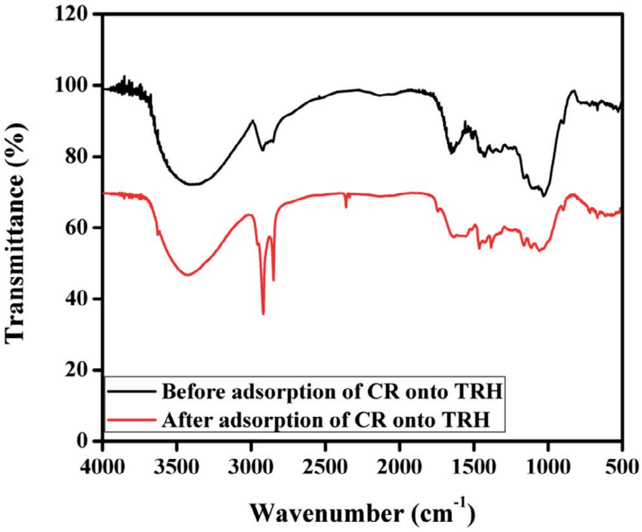

Fig. S3. FTIR spectra of MRH before and after adsorption of CR dye.

$$R_L = \frac{1}{1 + K_L C_o} \tag{S4}$$

The value of R_L represents the shape of the isotherm to be either unfavorable ($R_L > 1$), linear ($R_L = 1$), favorable ($0 < R_L > 0$), or irreversible ($R_L = 0$) [S4].

S2.2. Freundlich isotherm

Freundlich isotherm is an empirical relation used to discuss the heterogeneous system. It is given as [S5].

$$\log q_e = \log K_f + \frac{1}{n} \log C_e \tag{S5}$$

where K_f and n_F are Freundlich constant.

S2.3. Temkin isotherm

Temkin isotherm is in its linear form is expressed as [S6]:

$$q_e = B_T \ln A_T + B_T \ln C_e \tag{S6}$$

where $B_T = RT/b_T$, R is gas constant (8.31 J/mol K) and T is absolute temperature (K). The constant b_T is related to the heat of adsorption and A_T is equilibrium binding constant coinciding to the maximum binding energy.

S2.4. Dubinin–Radushkevich (D-R) isotherm

The Dubinin–Radushkevich (D-R) model is shown as [S6]:

$$\ln q_e = \ln q_m - \beta \varepsilon^2 \tag{S7}$$

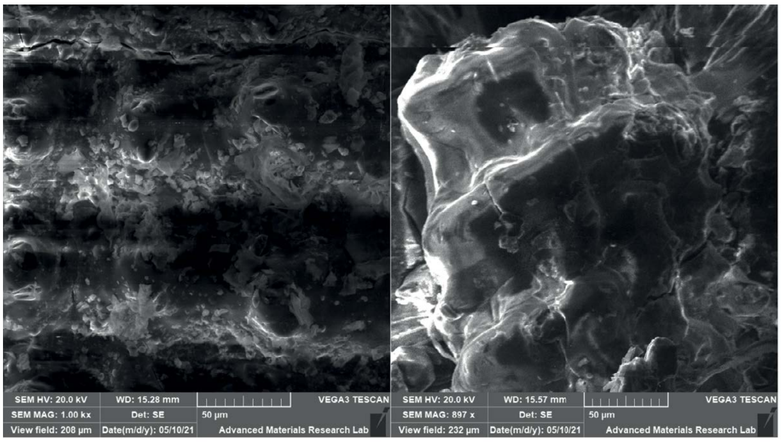

Fig. S4. (a) SEM micrographs of untreated rice husk (RH) and (b) NaOH treated.

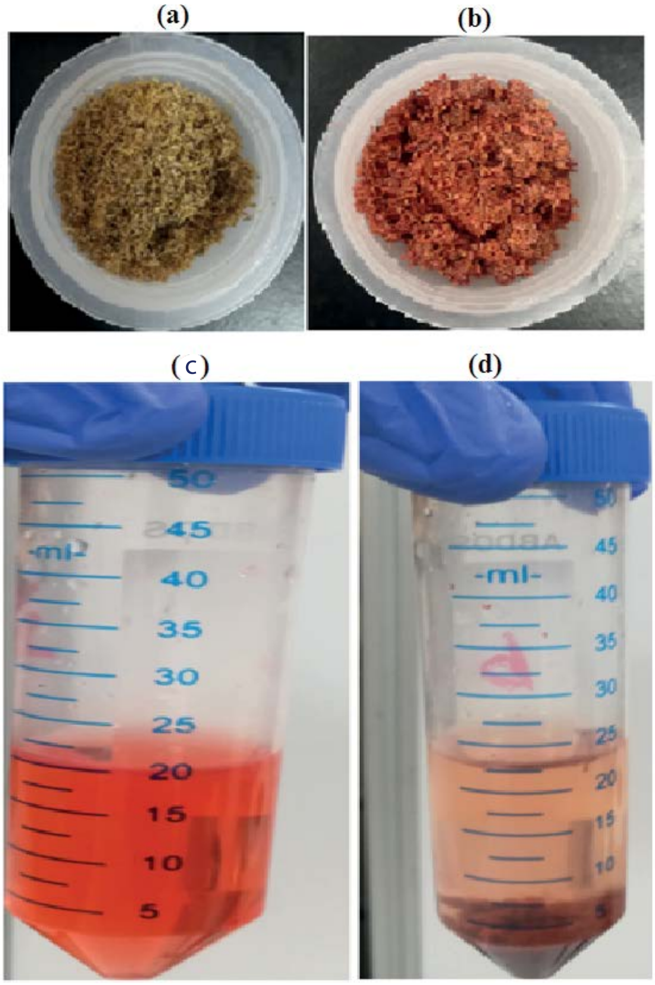

Fig. S5. (a) MRH before adsorption of CR, (b) MRH after adsorption of CR, (c) CR aqueous solution before adsorption onto MRH, and (d) CR aqueous solution after adsorption onto MRH.

where β (mol²/kJ) is constant related to adsorption energy and ε is the Polanyi potential can be recorded by using below relationship:

$$\varepsilon = RT\ln\left(1+\frac{1}{C_e}\right) \tag{S8}$$

where R is gas constant (8.31 kJ/mol) and T is absolute temperature (K). The below equation was used to determine the value of mean free energy E (kJ/mol):

$$E = \frac{1}{\sqrt{2\beta}} \tag{S9}$$

S3. Adsorption kinetics

S3.1. Pseudo-first-order model

The linear form of Lagergren pseudo-first-order rate in is expressed as [S7–S11]:

$$\log\left(q_e - q_t\right) = \log q_e - \frac{k_1 t}{2.303} \tag{S10}$$

where k_1 (min^{-1}), q_e and q_t denote rate constant of pseudo-first-order model, CR concentration adsorbed at equilibrium and time t respectively.

S3.2. Pseudo-second-order model

The linear form of pseudo-second-order kinetic model is given as [S10,S12]:

$$\frac{t}{q_t} = \frac{1}{k_2 q_e^2} + \frac{t}{q_e} \tag{S11}$$

where k_2 (g/mg min) is the rate constant of pseudo-second-order model.

S3.3. Elovich model

Elovich model is shown as [S13–S15]:

$$q_t = \frac{1}{\beta}\ln(\alpha\beta) + \frac{1}{\beta}\ln t \tag{S12}$$

where α (mg/g min) and β (g/mg) are constant. The parameter α is initial adsorption rate and β is the extent of surface coverage and activation energy for chemisorption.

S3.4. Modified Freundlich equation

It was originally presented by Kuo and Lotse [S12,S16]:

$$q_t = kC_o t^{1/m} \tag{S13}$$

where k, C_o, t and m are adsorption rate constant (L/g min), CR initial concentration (mg/L), contact time (min) and the Kuo–Lotse constant respectively. Its linear form is expressed as:

$$\ln q_t = \ln(kC_o) + \frac{1}{m}\ln t \tag{S14}$$

S3.5. Bangham equation

It is shown as [S10,S14]:

$$\log\log\left(\frac{C_o}{C_o - q_t m}\right) = \log\left(\frac{k_o m}{2.303V}\right) + \alpha \log t \tag{S15}$$

where m is mass of the MRH (adsorbent) employed (g/L), V is volume of CR dye aqueous solution (mL), α (<1) and k_o (mL/(g/L)) are constants.

S4. Adsorption thermodynamics

The below relationships were employed to record change in Gibb's free energy ($\Delta G°$), enthalpy ($\Delta H°$) and entropy ($\Delta S°$) to investigate adsorption thermodynamics for CR adsorption onto MRH as:

$$\ln K_c = \frac{\Delta S°}{R} - \frac{\Delta H°}{\mathrm{RT}} \tag{S16}$$

$$K_c = \frac{C_a}{C_e} \tag{S17}$$

$$\Delta G° = \Delta H° - T\Delta S° \tag{S18}$$

where K_c, $\Delta G°$, $\Delta H°$ and $\Delta S°$ are equilibrium constant, change in Gibb's free energy (kJ/mol), enthalpy (kJ/mol) and entropy (J/mol K) respectively.

References

[S1] I. Langmuir, The constitution and fundamental properties of solids and liquids, J. Franklin Inst., 183 (1917) 102–105.

[S2] I.W. Almanassra, V. Kochkodan, M. Subeh, G. McKay, M. Atieh, T. Al-Ansari, Phosphate removal from synthetic and treated sewage effluent by carbide derive carbon, J. Water Process Eng., 36 (2020) 101323.

[S3] T.W. Weber, R.K. Chakravorti, Pore and solid diffusion models for fixed-bed adsorbers, AlChE J., 20 (1974) 228–238.

[S4] G. McKay, Adsorption of dyestuffs from aqueous solutions with activated carbon I: equilibrium and batch contact-time studies, J. Chem. Technol. Biotechnol., 32 (1982) 759–772.

[S5] H. Freundlich, Uber die adsorption in lasugen (Leipzig), Z. Phys. Chem. A, 57 (1906) 385–470.

[S6] M.I. Khan, S. Zafar, M.A. Khan, F. Mumtaz, P. Prapamonthon, A.R. Buzdar, *Bougainvillea glabra* leaves for adsorption of congo red from wastewater, Fresenius Environ. Bull., 27 (2018) 1456–1465.

[S7] S. Zafar, M.I. Khan, M. Khraisheh, S. Shahida, T. Javed, M.L. Mirza, N. Khalid, Use of rice husk as an efective sorbent for the removal of cerium ions from aqueous solution: kinetic, equilibrium and thermodynamic studies, Desal. Water Treat., 150 (2019) 124–135.

[S8] M.I. Khan, S. Zafar, A.R. Buzdar, M.F. Azhar, W. Hassan, A. Aziz, Use of citrus sinensis leaves as a bioadsorbent for removal of congo red dye from aqueous solution, Fresenius Environ. Bull., 27 (2018) 4679–4688.

[S9] M.I. Khan, M.F. Azhar, A.R. Buzdar, W. Hassan, A. Aziz, M. Khraisheh, Leaves powder of syzgium cumini as an adsorbent for removal of congo red dye from aqueous solution, Fresenius Environ. Bull., 27 (2018) 3342–3350.

[S10] M.I. Khan, A. Shanableh, J. Fernandez, M.H. Lashari, S. Shahida, S. Manzoor, S. Zafar, A. ur Rehman, N. Elboughdiri, Synthesis of DMEA-grafted anion exchange membrane for adsorptive discharge of methyl orange from wastewaters, Membranes, 11 (2021) 166.

[S11] I.W. Almanassra, V. Kochkodan, G. McKay, M.A. Atieh, T. Al-Ansari, Kinetic and thermodynamic investigations of surfactants adsorption from water by carbide-derived carbon, J. Environ. Sci. Health, Part A, 56 (2021) 1206–1220.

[S12] M.I. Khan, M.H. Lashari, M. Khraisheh, S. Shahida, S. Zafar, P. Prapamonthon, A. Rehman, S. Anjum, N. Akhtar, F. Hanif, Adsorption kinetic, equilibrium and thermodynamic studies of Eosin-B onto anion exchange membrane, Desal. Water Treat., 155 (2019) 84–93.

[S13] M.A. Khan, M.I. Khan, S. Zafar, Removal of different anionic dyes from aqueous solution by anion exchange membrane, Membr. Water Treat., 8 (2017) 259–277.

[S14] M.I. Khan, S. Akhtar, S. Zafar, A. Shaheen, M.A. Khan, R. Luque, Removal of Congo Red from aqueous solution by anion exchange membrane (EBTAC): adsorption kinetics and themodynamics, Materials, 8 (2015) 4147–4161.

[S15] I.W. Almanassra, V. Kochkodan, G. McKay, M.A. Atieh, T. Al-Ansari, Review of phosphate removal from water by carbonaceous sorbents, J. Environ. Manage., 287 (2021) 112245.

[S16] M.I. Khan, J. Su, L. Guo, Development of triethanolamine functionalized-anion exchange membrane for adsorptive removal of methyl orange from aqueous solution, Desal. Water Treat., 209 (2021) 342–352.